Microwave properties of high-purity tetrathiofulvalene-tetracyanoquinodimethan (TTF-TCNQ)†

S. K. Khanna,* E. Ehrenfreund,‡ A. F. Garito, and A. J. Heeger
Department of Physics and Laboratory for Research on the Structure of Matter, University of Pennsylvania, Philadelphia, Pennsylvania 19174
(Received 21 November 1973)

An experimental study of the microwave properties of pure crystals of the organic salt tetrathiofulvalene-tetracyanoquinodimethan (TTF-TCNQ) is presented. Included are electron spin resonance and a complete study of the dielectric function, $\epsilon_1 - i\epsilon_2$, from room temperature to 4.2 K as measured along the principal conducting b axis and the transverse a axis using the highest-purity material synthesized thus far. The spin-resonance line is asymmetric characteristic of a metal with skin depth less than the sample thickness when the rf magnetic field is perpendicular to the b axis, and symmetric (Lorentzian) when the rf magnetic field is parallel to the b axis. These results are understood in terms of the Dyson-Bloembergen theory of resonance line shape as applied to the pseudo-one-dimensional metal. The dielectric measurements ($E||b$) are consistent with the skin-depth limiting behavior, and in the purest samples show negligible loss over a relatively wide temperature range ($50 < T < 100$ K) indicative of very high conductivity. Minimal attempts to reduce sample purity (no gradient sublimation and subsequent reaction in air) led to serious degradation of sample quality as evidenced by the appearance of significant loss throughout the entire metallic regime. The low-temperature dielectric constants appropriate to the b axis (ϵ_1^b) and a axis (ϵ_1^a) are found to be $\epsilon_1^b = (3.2 \pm 0.6) \times 10^3$ and $\epsilon_1^a = 6 \pm 2$. The value for ϵ_1^b is consistent with the known plasma frequency and energy gap. Studies of the temperature dependence of ϵ_1^b are used to obtain direct information on the energy gap in the low-temperature phase. The transport properties associated with the transverse (a axis) direction indicate an electrical anisotropy of 10^3 at room temperature increasing to about 10^4 near 60 K, thus confirming the picture of TTF-TCNQ as a highly anisotropic pseudo-one-dimensional metal. The a-axis transport is shown to be diffusive and severely limited as a result of the weak interchain coupling and the phonon thermal disorder. Evidence of excess low-temperature microwave conductivity in the purest samples at low temperatures is presented and discussed in terms of current models of the ground state.

I. INTRODUCTION

The transport properties of the organic charge-transfer salt tetrathiofulvalene-tetracyanoquinodimethan (TTF-TCNQ) [Fig. 1(a)] are of particular interest because this unique compound exhibits the highest electrical conductivity of any known organic system ($10^3\ \Omega^{-1}\,\mathrm{cm}^{-1}$ at room temperature).[1,2] As a result of the anisotropic chainlike structure[3] and the directional nature of the π molecular orbitals, the electronic properties of TTF-TCNQ are sufficiently anisotropic that this system may be regarded as a pseudo-one-dimensional metal.[4]

Conventional four-probe dc conductivity measurements along the crystallographic b axis indicate an unusually strong temperature dependence, with the conductivity increasing with decreasing temperature. Near 58–60 K, the conductivity goes through a relatively sharp maximum with typical values for the normalized conductivity ratio in the range from 10 to 20. Below the maximum, the conductivity falls dramatically, characteristic of a metal-insulator transition which has been associated with the Peierls instability.[1] The nonmagnetic ground state and nonenhanced susceptibility in the metallic state[4,5] demonstrated that Coulomb correlation effects play a minor role.[1,4] On the other hand, the electron-phonon interaction was found experimentally to be strong.[1,4,6–8] A pseudo-one-dimensional metal with strong electron-phonon interactions is expected to be unstable toward a Peierls soft-mode structural instability driven by the divergent response of the electron gas at $q = 2k_F$. In a general sense, one anticipates this would lead to a decrease in conductivity due to increased scattering from density fluctuations for a system approaching a phase transition. Thus, the strong temperature dependence observed in the metallic state has been difficult to understand on the basis of single-particle scattering. The fact that the conductivity above the transition increases rapidly with decreasing temperature in all samples was interpreted as evidence for the presence of electron pairing correlations mediated by the soft phonons near $2k_F$.[1] This interpretation led Bardeen[9] to point out that the correlations might indeed result from the Peierls effect; however, the resultant dynamically distorted state could give enhanced conductivity arising from the coupled electron-phonon running-wave mechanism first described by Fröhlich.[10] In principle, both pairing and the Fröhlich mechanism could be simultaneously operating since they do not appear to be mutually exclusive.[11] Recently, Allender, Bray, and Bardeen,[12] using a Ginsburg-

(a)

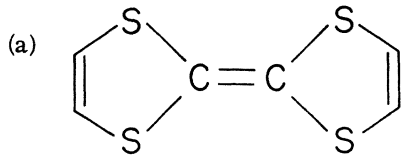

TTF

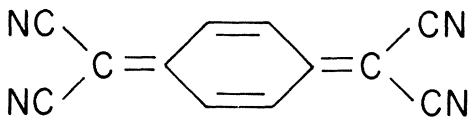

TCNQ

(b)

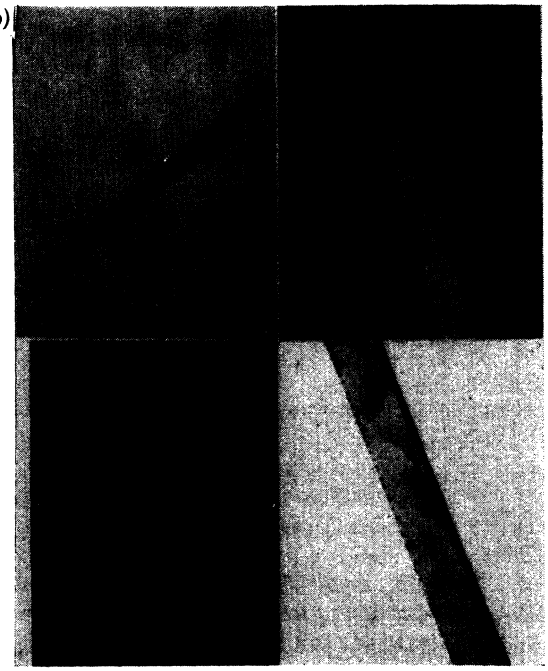

FIG. 1. (a) Molecular structure of TTF and TCNQ; (b) photographs of crystals of TTF-TCNQ having normal morphology with b axis parallel to crystal needle axis. The magnification is × 50 in the upper left, and × 100 for the other three.

Landau approach, have calculated a maximum normalized conductivity ratio of $\sigma/\sigma_{RT} \sim 10$ in agreement with the values commonly found for TTF-TCNQ (their results are limited to temperatures outside the critical region which they estimate as $\Delta T \sim 10$ K).

Evidence of strong correlations and excess dc conductivity in the metallic state above 60 K has been obtained from studies of the thermopower[13] and optical properties.[6-8] The thermopower deviates from the simple linear behavior found at high temperatures and approaches zero at the transition.[13] Considering the thermopower as a measure of entropy per carrier indicates a reduced entropy in the metallic state and strong electron-electron correlations in the temperature range ($60 < T < 140$ K) where the conductivity is maximum. Moreover, measurements of the temperature dependence of the scattering time τ from infrared reflectivity studies[6-8] provide evidence of excess dc conductivity and independently suggest that the steep temperature dependence of the conductivity in all TTF-TCNQ crystals arises not from single-particle scattering, but from a collective many-body effect. In a few samples, a giant conductivity peak has been observed and taken as evidence for the extreme sensitivity of pseudo-one-dimensional metals such as TTF-TCNQ to crystalline defects, twinning, and impurities.[1] However, it has been argued that conventional dc conductivity measurements can be misleading for highly anisotropic conductors, since one can assert that in spite of considerable care with the contacts, an inhomogeneous current distribution might be set up with nearly zero current density near the surface where the voltage contacts are made.[14] These experimental questions have been studied in detail with the conclusion that reliable dc conductivity measurements can be made.[15] Nevertheless, contactless microwave measurements are important to supplement the dc data.

Experimental studies of the microwave properties of TTF-TCNQ are important in the more general context of attempting to attain a detailed understanding of the fundamental physics involved in this unusual system. In this paper we present studies of the magnitude, anisotropy, and temperature dependence of the dielectric constant (ϵ_1) and the conductivity ($\epsilon_2 = 4\pi\sigma/\omega$) obtained from pure single crystals of TTF-TCNQ using the cavity perturbation technique of Buravov and Shchegolev.[16] These results are supplemented with spin-resonance studies, which provide independent evidence of high conductivity and show an asymmetric conduction-electron-spin-resonance line shape characteristic of a highly anisotropic (pseudo-one-dimensional) metal.

II. EXPERIMENTAL TECHNIQUES AND SAMPLE PREPARATION

A. Sample preparation

Tetracyanoquinodimethan (TCNQ) was prepared[17] under careful experimental conditions similar to those described in an earlier publication on N-methylphenazinium TCNQ.[18] Atomic absorption analysis of the resulting crystalline material gave less than 5-ppm alkali-metal impurity, while spin-resonance[19] and static-susceptibility[20] measurements indicate less than 1-ppm magnetic impurity. These results are consistent with recently completed photoconductivity studies[21] of the neutral

molecular crystal.

Tetrathiofulvalene (TTF) was prepared by generally following the method of Coffen and co-workers[22] in which 1, 3-dithiolium hydrogen sulfate or perchlorate is coupled using triethylamine.[23] The resulting dark brown TTF material was recrystallized from cyclohexane (Fisher spectrograde) yielding bright yellow-orange crystalline needles having excellent optical transparency. These were placed in a gradient sublimator which was lined with an inert DuPont "Kapton" sleeve, and pumped down to 1×10^{-5}–1×10^{-6} Torr. After sublimation was complete, significant fractionation was found to have taken place, with 20–40% of the total material accumulated as highly volatile forefraction material. Only the center zone material was collected and resublimed, yielding gemlike orange crystals as the center fraction; melting point is (119.3±0.1) °C in contrast to the earlier report of Wudl *et al.*[24] of (118.5–119) °C. Analysis: the calculated values for $C_6S_4H_4$ were C, 35.26; H, 1.98; S, 62.76; the values found were C, 35.25; H, 1.87; S, 62.71.

We conclude that the starting materials, the neutral TCNQ and TTF compounds, are ultrapure with active impurity levels on the scale of 10 ppm.

The TTF-TCNQ crystals were usually grown from solutions of multiply distilled CH_3CN using a U-tube diffusion technique, in a LabCon glove box filled with 99.999% Ar. Relatively slow growth occurred over a period of approximately 3 days, yielding lustrous black crystals which appeared yellow-brown upon inspection with an optical transmission microscope. Only smooth well-formed crystals with no crystal-plane steps or uneven edges were selected for use. Particular care was taken to choose crystals of excellent optical quality since the microwave measurements are particularly sensitive to steps and edges (depolarization fields inside the sample play an important role). An example is shown in Fig. 1(b). Typical crystal dimensions were $2\times0.2\times0.02$ mm. Analysis: The calculated values for $C_{18}H_8N_4S_4$ were C, 52.92; H, 1.98; N, 13.72; S, 31.39; the values found were C, 52.90; H, 2.08; N, 13.86; S, 31.35.

Independent experimental evidence of sample purity comes from the physical measurements themselves. For example, the magnetic susceptibility[20] of carefully prepared TTF-TCNQ shows a low-temperature Curie contribution ($\chi \propto T^{-1}$) indicative of only 0.01% (100 ppm) spin-$\frac{1}{2}$ impurities. If the Curie contribution were attributed to traces of transition metal (e.g., from the glassware) the corresponding concentration would be of order 10 ppm. The 0.01% ($S=\frac{1}{2}$) concentration is to be compared with the value of 0.07% reported by Perlstein *et al.*[25] for material synthesized by the Johns Hopkins group. The comparison with the Johns Hopkins material is particularly relevant, for microwave studies[26] on this material have been previously reported which are qualitatively different from those presented in this paper. The low-temperature spin susceptibility[20] in our samples is exponentially small, indicating a well-defined energy gap, in agreement with the heat capacity,[27] which shows no evidence of states in the gap. The most conclusive evidence to date of relative sample purity comes from measurements of the thermoelectric power. Chaikin *et al.*[13] have measured the thermopower of TTF-TCNQ in high-purity samples prepared in our laboratory and identical to those studied in this paper, and in samples prepared elsewhere with material known to be very impure.[28] Of particular interest is the low-temperature regime ($T<60$ K). The Penn samples showed a large positive thermopower, whereas the impure samples gave a large negative thermopower.[13] We make no attempt here at a detailed understanding of these results, but simply note that the negative thermopower is therefore an *empirical* signature of a high level of unknown donor impurities. Thermopower studies of the material synthesized and studied by Bloch *et al.*[26] show the same large negative thermopower observed in the purposely impure samples described above.[29] Therefore, their samples contain similar impurities at about the same level. This is consistent with the fact that in neither case was a gradient sublimation involved.[30] We conclude from the available evidence that the samples used in the present study are the best available, having impurity levels at least an order of magnitude lower than samples used in the microwave studies of Bloch *et al.*[26]

The typical crystal growth occurs with the long axis of the crystal coincident with the principal conducting (crystallographic b) axis of the solid. This was verified by the optical anisotropy and by independent x-ray studies. However, we have been able to obtain crystals with the long axis perpendicular to the b axis, and we report here measurements associated with the a-axis orientation. This orientation was again checked using polarized optical reflectivity and transmission, and x-ray measurements.

B. Experimental technique

The spin-resonance studies were performed on single crystals of TTF-TCNQ using a conventional Q-band (30 GHz) reflection spectrometer with a cylindrical cavity operating in the TE_{111} mode. The crystal orientation with respect to the fixed microwave magnetic field (H_1) was varied by manually rotating the crystal between field scans.

The dielectric constant (ϵ_1) and microwave conductivity ($\epsilon_2=4\pi\sigma/\omega$) measurements were carried out using the cavity perturbation technique of Bura-

vov and Shchegolev.[16] In this measurement one places the sample in the maximum electric field (antinode) of the cavity and determines the shift in cavity frequency (Δf) and change in half-width at half-maximum ($\frac{1}{2}\Delta$) resulting from the perturbation of the sample. The analysis assumes that the electric field inside the specimen can be determined from the static formula

$$E_i = E_0/[1+n(\epsilon-1)], \tag{1}$$

where E_0 is the unperturbed electric field in the cavity, $\epsilon = \epsilon_1 - i\epsilon_2$ the complex dielectric constant, and n the depolarization factor. It is important to note that Eq. (1) is valid only under conditions where the skin depth δ is greater than the sample thickness t,

$$\delta > t. \tag{2}$$

For higher conductivities, Eq. (1) is incorrect (the electric field falls exponentially inside the sample) and the dielectric formulation completely breaks down. We will see that for pure TTF-TCNQ this condition [Eq. (2)] is violated when the electric field is along the conducting b axis so that only a lower limit can be obtained for $\sigma_{\parallel}^{b}$. The depolarization factor can be estimated from the result expected for an ellipsoid of revolution,[31]

$$n = \frac{bc}{a^2}\left[\ln\left(\frac{4a}{b+c}\right)-1\right], \tag{3}$$

where a, b, and c are the semiaxes of the ellipsoid. Note that Eq. (3) can be used only as an estimate, for the actual samples necessarily have sharp edges and corners. We expect Eq. (3) to be accurate to better than a factor of 2 and find that where a direct independent experimental measurement can be made, Eq. (3) agrees with the experimental value (see below) to better than $\pm 50\%$.

The equations relating the change in half-width and the frequency shift to the dielectric functions are given by[16]

$$\tfrac{1}{2}\Delta_0 = \frac{\frac{1}{2}\Delta}{f_0} = \frac{\alpha\epsilon_2}{[1+n(\epsilon_1-1)]^2+(n\epsilon_2)^2}, \tag{4}$$

$$\Delta f_0 = \frac{\Delta f}{f_0} = \frac{\alpha\{(\epsilon_1-1)[1+n(\epsilon_1-1)]+n\epsilon_2^2\}}{[1+n(\epsilon_1-1)]^2+(n\epsilon_2)^2}, \tag{5}$$

where the filling factor $\alpha = \frac{1}{2}V_s E_{\max}^2/\int_{V_c}|E_0|^2\,dV$ (for a TE_{101} rectangular cavity $\alpha = 2V_s/V_c$), $E_{\max}$ is the magnitude of the electric field at the sample, V_s is the sample volume, V_c the volume of the cavity, and f_0 is the central frequency of the cavity. Solving for ϵ_1 and ϵ_2, one obtains

$$\epsilon_1 - 1 = \frac{1}{n}\left(\frac{\Delta f_0[(\alpha/n)-\Delta f_0]-(\frac{1}{2}\Delta_0)^2}{(\frac{1}{2}\Delta_0)^2+[(\alpha/n)-\Delta f_0]^2}\right), \tag{6}$$

$$\epsilon_2 = \frac{\alpha}{n^2}\left(\frac{\frac{1}{2}\Delta_0}{(\frac{1}{2}\Delta_0)^2+[(\alpha/n)-\Delta f_0]^2}\right). \tag{7}$$

From Eq. (5), we note that when the conductivity is large, $\epsilon_2 \gg \epsilon_1 \gg 1$, the shift is completely determined by sample geometry so that

$$\Delta f_0|_{\infty} = \alpha/n, \tag{8}$$

which provides an independent experimental measure of the depolarization factor.[16]

The experimental apparatus utilized a rectangular cavity operating in the TE_{101} transmission mode with an operating frequency of 10.4 GHz. The sample holder consisted of a slotted styrofoam pellet which was inserted into a thin-wall polystyrene tube connected to a simple gear arrangement which allowed manual turning of the sample from outside the cryostat. The styrofoam pellet was trimmed so that there was no detectable shift on rotation with no sample in the cavity. With the sample needle axis perpendicular to the cavity E field, the depolarization factor is of order unity, resulting in no observable shift and minimal loss of Q. Typically, data were taken at each temperature by recording the cavity transmission with sample needle axis first parallel and then perpendicular to the cavity E field. The results from the perpendicular orientation were taken as characteristic of the bare cavity. This was checked independently by using a plunger arrangement which actually removed the sample from the cavity. The results indicated that the somewhat easier parallel-perpendicular comparison involved negligible error for all quantities reported in this paper. The microwave power was obtained from a H-P 8690B sweep oscillator operated at low rf level (approximately 1 μW) to ensure against sample heating. The cavity was pressurized with 1 atm of He exchange gas, and we estimate a maximum sample power absorption of 20 nW for crystals oriented with conducting axis along the needle axis, and 200 nW for the transverse crystals. The results were insensitive to an order-of-magnitude increase in power. The transmitted signal was detected by a calibrated microwave crystal diode operating in the square-law region (less than 40 μV maximum). To obtain good signal to noise at these low levels, the rf power was amplitude modulated (1 kHz) and the resulting ac signal was demodulated with a lock-in amplifier. The output of the lock-in was recorded directly on an xy recorder from which the shift and change in width could be read. By careful calibration of the frequency sweep, the shift could be determined with an absolute accuracy of ± 10 kHz and the change in width with an absolute accuracy of ± 10 kHz. Although more sophisticated measurements of the change in cavity Q can be envisioned, the above technique is straightforward and the accuracies were sufficient for all measurements reported here.

As an independent check on the technique, the

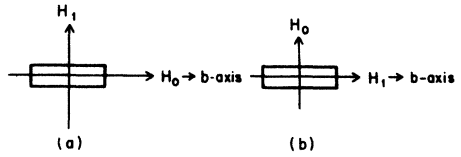

FIG. 2. Crystal orientation relative to the microwave field (H_1) and the static magnetic field (H_0) in the ESR experiment. (a) H_1 perpendicular to crystal b axis; (b) H_1 parallel to crystal b axis.

dielectric constants of single crystals of N-methyl-phenazinium TCNQ (NMP-TCNQ) and potassium TCNQ were measured and found to be $\epsilon_1(7\text{ K}) = 350 \pm 50$ and $\epsilon_1(300\text{ K}) = 7 \pm 2$, in good agreement with the results reported by Buravov *et al.*[32] and Vlasova *et al.*,[33] respectively.

III. EXPERIMENTAL RESULTS

A. Electron spin resonance

Our purpose here is to present independent experimental evidence from electron-spin-resonance measurements that, for the TTF-TCNQ crystals used in this study, the metallic conductivity along the crystal b axis is in the classical skin-effect regime throughout the temperature range 60–300 K.

When the skin depth is comparable to or less than the metal sample thickness t, the spin-resonance line shape is asymmetric and governed by the ratio $(T_D^{\perp}/T_2)^{1/2}$, where $T_D^{\perp}$ is the time taken for an average spin to diffuse in the direction normal to the surface through a distance equal to the skin depth, and T_2 is the electron spin-spin relaxation time.[34] The classical skin effect limits penetration of the microwave field into the metal to the skin depth given as usual by

$$\delta = c/(2\pi\sigma\omega)^{1/2}, \tag{9}$$

where c is the velocity of light and σ is the conductivity. Since the conductivity is anisotropic, the skin depth is expected to be similarly anisotropic. We show, for example, two configurations in Fig. 2. For case (a), the microwave magnetic field is perpendicular to the b axis so that σ_b would enter into Eq. (9). For case (b), the transverse conductivity determines the skin depth.

The room-temperature spin-resonance line for TTF-TCNQ (sample dimensions $2.6 \times 0.30 \times 0.03$ mm) is shown in Fig. 3. In Fig. 3(a), the crystal is oriented as in case (a) (Fig. 2), where the H_1 microwave field is perpendicular to the conducting b axis, thereby inducing currents inside the metal along the b axis. The observed Dyson-Bloembergen asymmetric line shape clearly indicates that the skin depth associated with the b axis, $\delta_{\parallel}$, is indeed less than t. Since the field can penetrate from either side, we conclude that $\delta_{\parallel} < 15\ \mu$m.

Using this value for δ in Eq. (9), the conductivity along the b axis is calculated to be $\sigma_{\parallel}^{b} > 500\ (\Omega\,\text{cm})^{-1}$, in agreement with the dc[1,15] and optical results[6–8] obtained on pure samples in previous studies. The measured value of $A/B = 2.5 \pm 0.5$ corresponds to the Bloembergen limit of Dyson's line-shape equations, where $T_D^{\perp}$ is quite long (the peak heights A and B are defined in Fig. 3). In TTF-TCNQ, $T_D^{\perp}$, which is in the transverse direction, is expected to be long as a result of the weak coupling between chains. As estimate of $T_D^{\perp}$ based on the transverse conductivity measurements presented in this paper indicates $T_D^{\perp}/T_2 \sim 10^6$.

For the highly anisotropic pseudo-one-dimensional metal TTF-TCNQ, the magnitude of the conductivity transverse to the principal conducting axis is nearly three orders of magnitude smaller. As a further check, the spin-resonance line is presented in Fig. 3(b), where H_1 is parallel to the conducting b axis as in case (b) (Fig. 2). As expected, the line is symmetric, Lorentzian, and non-skin-depth-limited.[35]

The characteristic asymmetry shown in Fig. 3(a) is not always obtained in room-temperature studies. Poorer quality crystals do show symmetric lines at room temperature, and the appearance of asymmetry can be used as an indicator of sample quality. We note, however, that even for crystals which

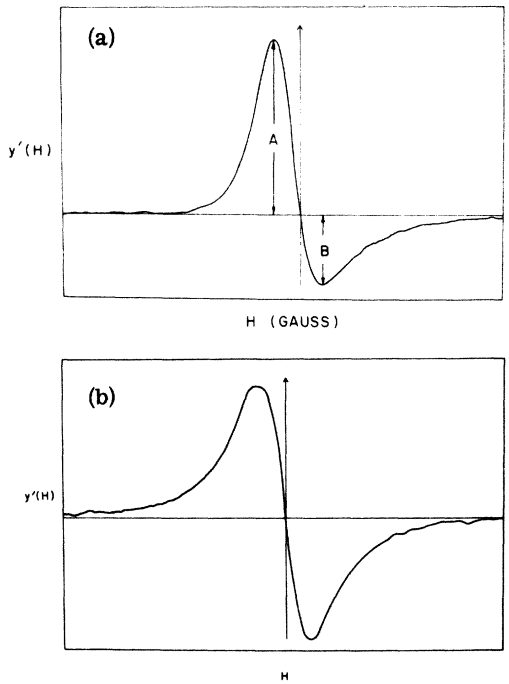

FIG. 3. First derivative of the ESR absorption line of TTF-TCNQ at room temperature (30 GHz). (a) Microwave field (H_1) perpendicular to the b axis as in Fig. 2(a). The sweep width is 50 G. (b) Microwave field (H_1) parallel to b axis as in Fig. 2(b). The sweep width is 50 G.

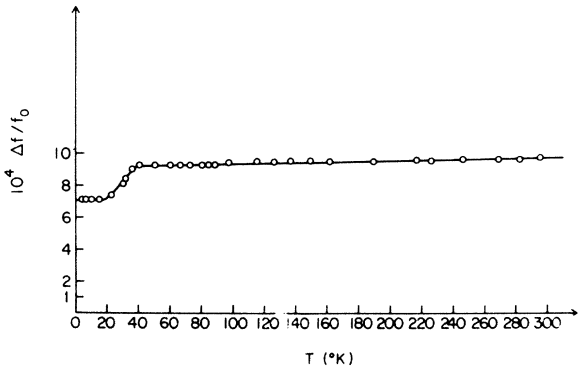

FIG. 4. Temperature dependence of the cavity frequency shift ($\Delta f/f_0$) with E parallel to crystal b axis.

showed symmetric lines, on cooling below room temperature $\sigma_{\parallel}^{b}$ increased sufficiently that the characteristic asymmetry appeared, indicating skin-depth-limited behavior.

That the spin-resonance signals are intrinsic to the electronic structure of TTF-TCNQ and not, say, to extrinsic localized spins in the metal samples has been established by carrying out quantitative spin-resonance studies at 30 MHz[20] using the Schumaker-Slichter technique.[36] The spin susceptibility directly determined from spin resonance agrees with the static susceptibility measured by the usual Faraday method.[20] A detailed experimental study of the spin-resonance linewidth and line shape as a function of temperature will be presented elsewhere.[37]

B. Microwave dielectric constant ($\epsilon_1 - i\epsilon_2$) with $E \parallel b$

The high dc conductivity along the b axis together with Eq. (9) for the skin depth imply that the Shchegolev dielectric technique[16] may be inapplicable to high-purity TTF-TCNQ. This difficulty is confirmed by the observation of the Dyson line shape in the spin resonance which demonstrates that $\delta_{\parallel} < t$.

Independent evidence of high conductivity and the breakdown of Eq. (2) is obtained from the experimental measurements of the shift in cavity resonance frequency, Δf_0, and the comparison of these results with Eq. (5). The normalized shift versus temperature is shown in Fig. 4. Of particular interest is the metallic regime, $T > 60$ K. Throughout this regime we find that Δf_0 decreased monotonically with decreasing temperature. This is contrary to the expected behavior based on Eq. (5).

We can estimate ϵ_2^b from the known dc results. Using $\epsilon_2 = 4\pi\sigma/\omega$ and $\sigma_{\parallel}^{b}(\mathrm{RT}) > 500\ (\Omega\,\mathrm{cm})^{-1} = 5\times10^{14}$ sec^{-1}, one finds $\epsilon_2^b(\mathrm{RT}) > 10^5$. Moreover, there is general agreement from dc studies that σ increases by more than an order of magnitude as the temperature is lowered toward 60 K. Thus, over the entire metallic regime, we assume $\epsilon_2^b > 10^5$. Examination of Eq. (5) shows that if $\epsilon_2 \gg |\epsilon_1| \gg 1$, the shift has the simple form given in Eq. (8). Moreover, as ϵ_2 *increases*, Δf_0 should increase approaching the value $\Delta f_0|_{\infty} = \alpha/n$ asymptotically. One might question the condition $\epsilon_2 > |\epsilon_1|$; however, from simple theory one expects for a metallic system at low frequency ($\omega < 1/\tau$)

$$\epsilon_1 \simeq 1 - \omega_p^2\tau^2 . \tag{10}$$

The quantities ω_p and τ have been measured independently for TTF-TCNQ[6-8] ($E \parallel b$) with the result that $\omega_p\tau \simeq 10$ in the metallic regime, so that $|\epsilon_1| \sim 10^2$, i.e., three orders of magnitude less than the value of ϵ_2 estimated above.

The inconsistency of Eqs. (5) and (8) with the experimental cavity-frequency-shift measurements thus provides independent evidence of high conductivity and the breakdown of Eq. (2). The dielectric formulation of the cavity perturbation problem is thus invalid, and $\delta_{\parallel} \ll t$. We conclude, therefore, that for high-purity TTF-TCNQ the microwave conductivity along the principal b axis is too large to be analyzed by the Buravov-Shchegolev dielec-

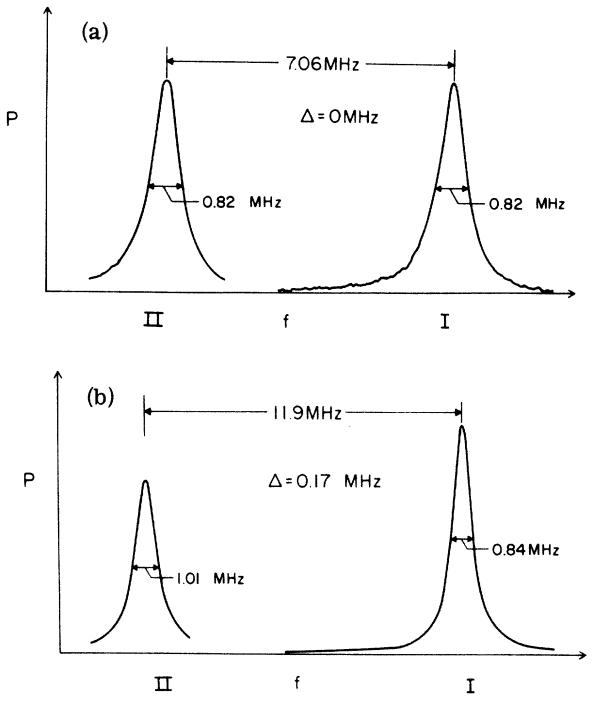

FIG. 5. Effect of sample purity on the microwave conductivity. The transmitted power (P) is plotted versus frequency (f) at 77 K: (a) High-purity sample exhibiting no detectable loss, (I) E field perpendicular to crystal and b axes, (II) E field parallel to crystal and b axes; (b) less-pure sample exhibiting microwave losses, (I) E field perpendicular to crystal and b axes, (II) E field parallel to crystal and b axes.

TABLE I. Dielectric constants ($\epsilon = \epsilon_1 - i\epsilon_2$) measured parallel to b axis at low temperature for pure (1-5) and impure (6-10) crystals (see text) of TTF-TCNQ. The associated filling (α) and depolarization (n) factors are related to the frequency shift (Δf_0) by Eq. (8), where $\Delta f_0|_\infty$ and Δf_0 (low T) were obtained at room and low temperatures, respectively.

S No.	α	n_{expt}	n_{th}	$\Delta f_0\|_\infty$	Δf_0(low T)	ϵ_1	$\epsilon_2 = 4\pi\sigma/\omega$
1	8.78×10^{-7}	9.0×10^{-4}	6.0×10^{-4}	9.69×10^{-4}	7.09×10^{-4}	3.03×10^{3}	1×10^{2}
2	1.94×10^{-6}	1.4×10^{-3}	1.1×10^{-3}	1.35×10^{-3}	1.14×10^{-3}	3.9×10^{3}	44
3	4.65×10^{-7}	1.4×10^{-3}	1.6×10^{-3}	3.35×10^{-4}	2.92×10^{-4}	4.3×10^{3}	4.2×10^{2}
4	9.14×10^{-7}	2.4×10^{-3}	1.6×10^{-3}	3.81×10^{-4}	3.12×10^{-4}	2.0×10^{3}	84
5	6.78×10^{-7}	1.10×10^{-3}	6.2×10^{-4}	5.98×10^{-4}	4.55×10^{-4}	2.8×10^{3}	86
6	4.27×10^{-6}	3.2×10^{-3}	2.3×10^{-3}	1.31×10^{-3}	1.1×10^{-3}	2.4×10^{3}	<5
7	2.3×10^{-6}	3.1×10^{-3}	2.6×10^{-3}	7.36×10^{-4}	6.35×10^{-4}	2.1×10^{3}	<5
8	1.56×10^{-6}	3.54×10^{-3}	2.76×10^{-3}	4.4×10^{-4}	3.75×10^{-4}	2.2×10^{3}	<5
9	3.1×10^{-6}	2.71×10^{-3}	2.1×10^{-3}	1.14×10^{-3}	9.4×10^{-4}	1.7×10^{3}	<5
10	1.71×10^{-6}	4.3×10^{-3}	2.75×10^{-3}	3.97×10^{-4}	3.44×10^{-3}	1.6×10^{3}	<5

tric formulation, and only a lower limit can be set for the value of $\sigma_{\parallel}^{b}$.

Figure 5(a) shows the actual recorder traces of cavity transmission for a single crystal of high-purity TTF-TCNQ at 77 K. The cavity Q is identical (to within experimental error) for the crystal parallel and perpendicular to the rf electric field; i.e., we are unable to detect a significant loss for $E \parallel b$. We have purposely attempted to make TTF-TCNQ of somewhat poorer quality as a check on these results. The material was synthesized in the usual manner, but the final gradient sublimation steps were not carried out, and the final reaction to the salt was performed in air (see Sec. III D). Figure 5(b) shows the cavity transmission data for such a crystal; one clearly sees a decreased Q (i.e., significant loss).

The spin-resonance results and estimates based on the dc conductivity indicate that at room temperature $\delta_{\parallel} \sim t$, so that a meaningful estimate for the microwave conductivity might be obtained from the room-temperature change in half-width. Analysis of the data for the best material yields $\sigma_{\parallel}^{b}(\mathrm{RT}) \geq 500\ (\Omega\,\mathrm{cm})^{-1}$, with 10^3 being the largest we have observed. The results are in agreement with the dc room-temperature values which regularly yield values between 500 and $10^3\ (\Omega\,\mathrm{cm})^{-1}$.[1]

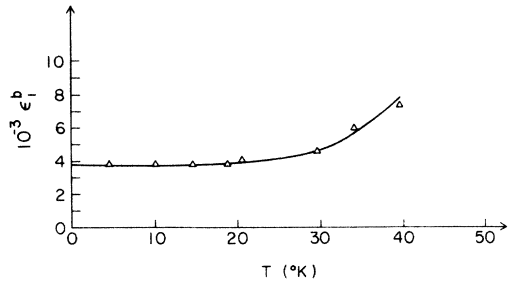

FIG. 6. Temperature dependence of the dielectric constant ϵ_1^b measured along the b axis.

Below 60 K, the conductivity decreases dramatically as a result of the metal-insulator transition. One therefore expects Eq. (2) to be easily fulfilled. This is confirmed by the observation of symmetric spin-resonance lines in this regime.[37] The low-temperature frequency shift is shown in Fig. 4. In the vicinity of 60 K, there is a change in slope, with Δf_0 decreasing toward a low-temperature constant value. Qualitatively, the shift remains large, indicating a significant field perturbation and therefore a relatively large dielectric constant.

The low-temperature dielectric-constant (ϵ_1^b) measurements are summarized in Table I and Figs. 6 and 7. Table I provides the relevant data for several specimens giving the filling factor (α), the theoretical value of the depolarization factor (n), and the experimental value of n as obtained from $\Delta f_0|_\infty = \alpha/n$ and the room-temperature shift. Note that in all cases n_{th} and n_{expt} are in agreement to $\pm 50\%$, with the deviations probably arising from edge and corner effects due to the nonellipsoidal shape of the specimens.

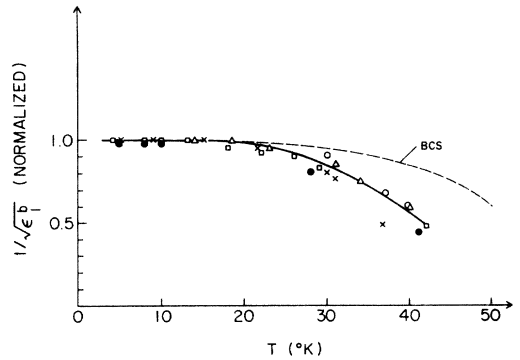

FIG. 7. Temperature dependence of $(\epsilon_1^b)^{-1/2}$ for several crystals. The results are normalized to the low-temperature value. The mean-field (BCS) gap dependence is shown for comparison.

Figure 6 shows the temperature dependence of ϵ_1^b for one sample in the insulating regime ($T < 40$ K). The low-temperature value is 4000 and increases dramatically as T increases toward the metallic state. A summary of results for ϵ_1^b (low T) is given in Table I. The first five samples listed in Table I are high-purity TTF-TCNQ characteristic of the best material we have synthesized thus far, giving $\epsilon_1^b = 3.2 \pm 0.7 \times 10^3$. The latter five are less pure, deriving from material which was not gradient sublimed and was subsequently reacted in air (see Sec. III D). The less-pure samples give somewhat lower values for the low-temperature dielectric constant [$\epsilon_1^b = (2.0 \pm 0.3) \times 10^3$]. Figure 7 shows the (normalized) data for several samples plotted as $(1/\epsilon_1^b)^{1/2}$ versus T. There is some scatter from sample to sample, but the over-all trend is clear.

The low-temperature insulating phase of TTF-TCNQ is that of a small-band-gap nonmagnetic semiconductor. The suggestion of a gross change in charge transfer [back to the neutral TTF and TCNQ or to the doubly ionized $(TTF)^{++}(TCNQ)^{--}$ configuration][2,26] has been ruled out by the observation that the plasma frequency ω_p^b is independent of temperature.[6-8]

The dielectric constant of a small-band-gap one-dimensional semiconductor is presented in tight-binding theory in the Appendix. The result is given by

$$\epsilon_1^b = 1 + 0.65(\omega_p^b/\omega_G)^2 , \tag{11}$$

where $\omega_p^b = (4\pi N e^2/m_b^*)^{1/2}$ is the plasma frequency associated with the principal conducting axis and m_b^* is the optical effective mass associated with the transfer along this axis. $(\hbar\omega_G)$ is the minimum (direct) semiconducting energy gap. A similar result was derived by Rice and Strässler[38] using a constant-density-of-states model [$\epsilon_1 = 1 + \frac{1}{3}(\omega_p^2/\omega_G^2)$], and by Lee, Rice, and Anderson[39] [$\epsilon_1 = 1 + \frac{2}{3}(\omega_p^2/\omega_G^2)$].

The plasma frequency has been determined (for $E \parallel b$) from polarized reflectivity studies in the infrared on single crystals of TTF-TCNQ.[6-8] A Drude analysis yields $(\hbar\omega_p^b) = 1.2$ eV. Direct measurements of the semiconducting energy band gap are not available. However, information on the magnitude of the gap can be obtained from the exponential dependence of the conductivity,[1] magnetic susceptibility,[20] and nuclear relaxation rates.[40] A value of $E_g/k_B = 120$ K has been inferred from the conductivity data[2] (note that one expects $\sigma \propto e^{-E_g/2kT}$). However, the plots of $\ln\sigma$ versus T^{-1} are not straight and this value might be questioned. The low-temperature spin susceptibility[20] is exponential in T^{-1}, and yields a single-particle energy gap of $E_g/k_B \simeq 150$ K, and the proton relaxation rate below 50 K is consistent with this value.[40] Thus, we conclude that $E_g/k_B \simeq 150$ K at low temperatures

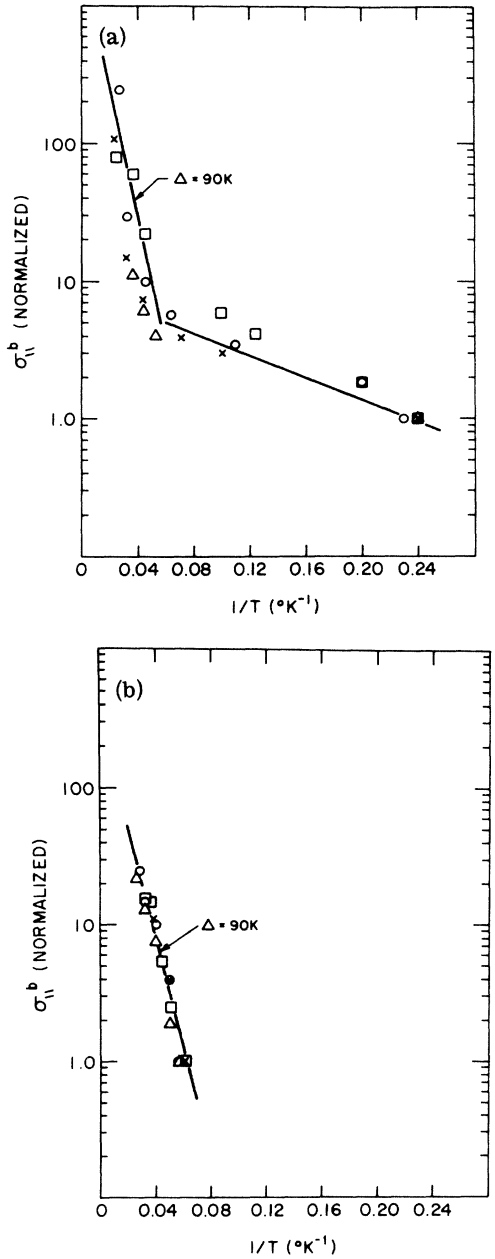

FIG. 8. Microwave conductivities of pure and impure (see text) crystals of TTF-TCNQ along the b axis. The data were normalized to the low-temperature value. (a) $\log\sigma$ (normalized) versus T^{-1} for purest crystals available; (b) $\log\sigma$ (normalized) versus T^{-1} for crystals derived from nongradient sublimed material and reacted in air.

with an estimated uncertainty of ±30 K. Using these values for ω_p^b and $\hbar\omega_G = E_g$, one finds from Eq. (11)

$$\epsilon_1^b = 1 + 0.65(\omega_p^b/\omega_G)^2 \simeq 4000 , \tag{12}$$

in excellent agreement with the measured value $(3.2 \pm 0.7) \times 10^3$.

The temperature dependence of the b-axis conductivity for $T < 40$ K is shown in Fig. 8. Figure 8(a) shows the normalized values of $\ln\sigma_{\parallel}^{b}$ versus T^{-1} for high-purity samples (absolute values are given in Table I). The conductivity decreases exponentially as a function of T^{-1} with $\Delta/k_B = E_g/2k_B \simeq 90$ K and then flattens to a nearly constant low temperature which is nearly four orders of magnitude greater than the dc conductivity at 4.2 K. There is no intrinsic disorder in TTF-TCNQ to cause the frequency dependence as observed in amorphous materials. However, with a dielectric constant of order 3×10^3, impurity ionization potentials might be expected to be extremely small so that trace impurities could dominate the conductivity at low temperatures.[41] The effects of impurities are considered below and are found to have just the opposite effect of supressing the excess low-temperature conductivity. On the other hand, the pinned giant density wave conductivity of Lee, Rice, and Anderson[39] would be expected to be frequency dependent and largest in pure samples.

C. Microwave dielectric constant $(\epsilon_1 - i\epsilon_2)$ with $E \perp b$

We have been able to grow single crystals of TTF-TCNQ in the form of long needles (with typical dimensions $2\times0.18\times0.007$ mm) with the b axis perpendicular to the needle axis which is coincident with the crystallographic a axis. This orientation was checked using the anisotropic optical transmission of polarized light, and with x-ray techniques. X-ray powder patterns were also studied to assure against an unknown second phase.

The cavity shift and change in half-width versus temperature for $E \parallel a$ are shown in Figs. 9 and 10. Note particularly that the shift is relatively small and increases with decreasing temperature, then goes quickly to a very small low-temperature value. In contrast to the $E \parallel b$-shift data in Fig. 4,

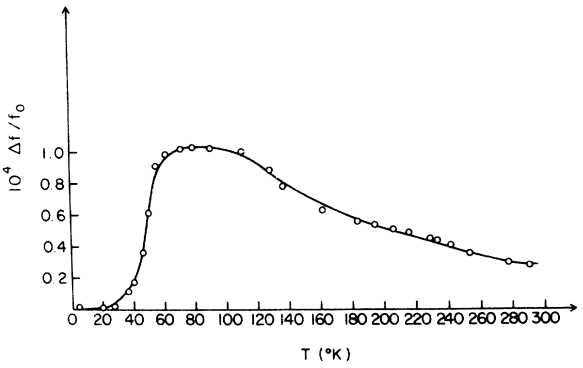

FIG. 9. Temperature dependence of the cavity frequency shift $(\Delta f/f_0)$ with E along the crystal a axis.

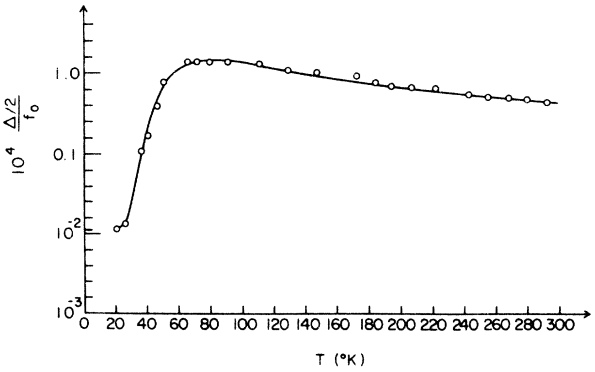

FIG. 10. Temperature dependence of the change in cavity half-width at half-maximum $(\frac{1}{2}\Delta)/f_0$ with E along the crystal a axis.

for the perpendicular configuration, the shift versus temperature is consistent with expectations based on the dielectric formulation and Eq. (5). Analysis of the data using Eqs. (6) and (7) and the theoretical value of α/n (obtained from the sample dimensions) leads to the temperature dependence of σ_1^a and ϵ_1^a shown in Figs. 11 and 12.

The room-temperature microwave conductivity $\sigma_{\perp}^{a}(\mathrm{RT}) = 0.5\ (\Omega\,\mathrm{cm})^{-1}$, indicating an anisotropy, $\sigma_{\parallel}^{b}/\sigma_{\perp}^{a}|_{\mathrm{RT}} \gtrsim 10^3$. The microwave $\sigma_{\perp}^{a}(T)$ is seen to increase smoothly with decreasing temperature with a maximum value (at 75 K) of 2.4 times the room-temperature value. The dc conductivity[15] along this axis is shown for comparison as the solid curve in Fig. 11. The agreement between the dc and 10-GHz data is excellent over the entire temperature range. Below 30 K, $\sigma_{\perp}^{a}$ quickly drops below $10^{-2}\ (\Omega\,\mathrm{cm})^{-1}$ and becomes undetectable as loss in the cavity.

The dielectric constant ϵ_1^a remains positive over the entire temperature range from 4.2 to 300 K as shown in Fig. 12. This is particularly interesting in the context of the known metallic behavior along the principal conducting b axis, and the observed negative temperature coefficient for $\sigma_{\perp}^{a}(T)$ shown in Fig. 11. The positive values found for $\epsilon_1^a(T)$ provide strong evidence that the description of the transport along the a axis is *not* that of simple metallic behavior even in the "metallic" regime above 60 K where there is strong evidence of a degenerate electron system. The dielectric constant at low temperatures is quite small, $\epsilon_1^a \simeq 6$, indicating an anisotropy, $\epsilon_1^b/\epsilon_1^a = 500$. This remarkable result is again strong evidence of the pseudo-one-dimensionality of TTF-TCNQ.

The large anisotropy in ϵ_1 and the associated small value along the a axis are not surprising in view of the expected small transfer integral associated with the interchain coupling. As a result,

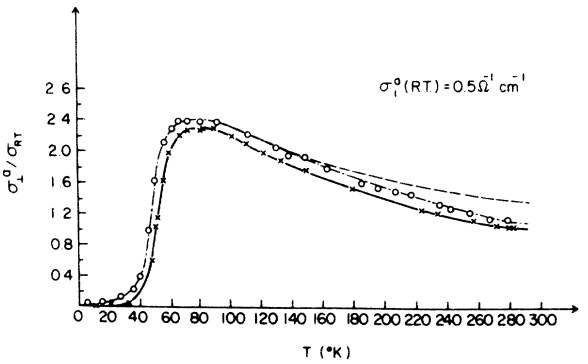

FIG. 11. Temperature dependence of the conductivity (σ_1^a) along the *a* axis: dash–open-line, 10.4 GHz; dash-cross line, dc. The dashed curve shows a $T^{-1/2}$ dependence for comparison.

the oscillator strength and polarizability along *a* are small, leading to a small dielectric constant.

D. Effect of nonspecific impurities and comparison with other results

The first of a series of planned studies of the effects of impurities on the properties of TTF-TCNQ has been completed. Samples were purposely grown in air using unsublimed TTF and TCNQ and, in some cases, unpurified acetonitrile solvent.

In each case, the resulting low-temperature value of ϵ_1^b was lower $[(2.0 \pm 0.3) \times 10^3]$ and the excess low-temperature microwave conductivity was absent compared to the values for highly purified samples. Impure samples are listed as 5–10 in Table I and the temperature dependence of the measured conductivity $\sigma_{\parallel}^b$ for $T < 60$ K is given in Fig. 8(b), showing that exponential dependence is observed as for the pure samples, but the excess low-temperature conductivity is absent. Agreement in chemical analyses with the TTF-TCNQ stoichiometry was obtained for each sample. Thus, small amounts of nonspecific chemical impurities introduced by improper materials preparation procedures chemically degrade the low-temperature values of ϵ_1^b and $\sigma_{\parallel}^b$.

In contrast to the pure samples of TTF-TCNQ, the impure samples exhibit significant loss for $E \parallel b$ [Fig. 5(b)]. This behavior is similar to that described by Bloch *et al.*[26] They indicate that the skin depth was not a limitation in their experiments, that significant loss was observed throughout the metallic regime, and that at no time did they observe the narrow cavity resonance and large cavity shift characteristic of a sample with skin depth much less than the sample thickness. Moreover, they did not observe the excess low-temperature microwave conductivity, but found near agreement between the dc and microwave results.

It is instructive to compare the ϵ_1 results obtained here on normal, transverse, and impure samples with the previous result, $\epsilon_1 \simeq 50$, reported by Bloch *et al.*[26] Given the values $\epsilon_1^b = (3.2 \pm 0.7) \times 10^3$ and $\epsilon_1^a \simeq 6$, then in a sample exhibiting mixed normal and transverse habits, the smaller dielectric constant ϵ_1^a would tend to dominate. As a test, ϵ_1 was determined for a polycrystalline pressed pellet and a composite sample consisting of a normal crystal placed in series with a transverse crystal. For the polycrystalline sample $\epsilon_1 \simeq 120$, and for the composite sample $\epsilon_1 \simeq 180$.

In a further attempt to chemically degrade the low-temperature ϵ_1^b to lower values, it was found that samples grown from ultrapure TTF and TCNQ in acetonitrile solvent containing small amounts of water gave values of $\epsilon_1^b \simeq 500$.

Since Bloch *et al.*[26] reported values of ϵ_1 for NMP-TCNQ in agreement with literature values and with those obtained for NMP-TCNQ in this study, we are led to conclude that their smaller low-temperature ϵ_1 values result not from differences in measurement technique but from chemical or crystallographic inhomogeneities present in their samples. This is consistent with the finding discussed above that other physical properties of their material, such as the thermopower, were the same as those of known impure samples.[13,29]

IV. DISCUSSION OF RESULTS

The principal experimental results which define the microwave properties of high-purity TTF-TCNQ are summarized below.

(a) The Dyson-Bloembergen line shape for rf field (H_1) is perpendicular to the *b* axis [Fig. 3(a)].

(b) There is an anomalous shift versus temperature for $E \parallel b$ (Fig. 4).

(c) Negligible loss was found (in cavity) over a wide temperature range ($50 < T < 100$ K) in pure material for $E \parallel b$.

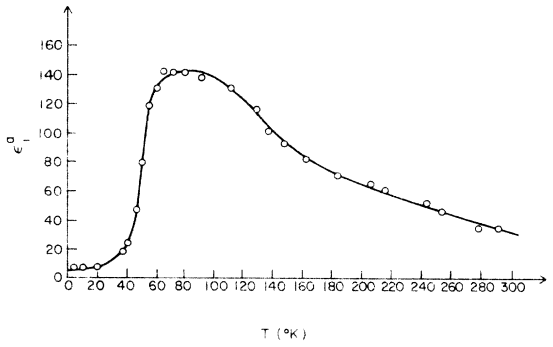

FIG. 12. Temperature dependence fo the *a*-axis dielectric constant (ϵ_1^a).

(d) There is a large low-temperature dielectric constant, $\epsilon_1^b \simeq 3200$, which increases as $T \to 60$ K (Fig. 6 and Table I).

(e) There is finite microwave conductivity at low temperature along the b axis in pure crystals (Fig. 8).

(f) There is a symmetric Lorentzian line shape for the rf field (H_1) parallel to the b axis (Fig. 3(b)].

(g) The small magnitude and relatively weak temperature dependence of $\sigma_1^a(T)$ in the "metallic" regime indicates a room-temperature anisotropy of order 10^3 (Fig. 11).

(h) A small low-temperature dielectric constant, $\epsilon_1^a = 6$, was found along the a axis (Fig. 12).

(i) $\epsilon_1^a(T)$ is positive and temperature dependent in the "metallic" regime (Fig. 12).

Properties (a), (b), and (c) have been discussed in some detail above. Together they provide strong evidence of high conductivity along the b axis, with the associated skin depth $\delta_{\parallel}$ much less than the sample thickness over the entire metallic regime. The room-temperature value is approximately $\sigma_{\parallel}^b(\mathrm{RT}) = 10^3\ (\Omega\,\mathrm{cm})^{-1}$. These results are in contrast with the data of Bloch *et al.*[26] which show no evidence of small skin depths and show significant loss at all temperatures.

The large dielectric constant at low temperatures for $E \parallel b$ follows naturally from the known plasma frequency and energy gap for this crystallographic direction. Given this interpretation, the temperature dependence of $(\epsilon_1^b)^{-1/2}$ as shown in Fig. 7 provides a measure of the temperature dependence of the energy gap. Assuming a simple mean-field treatment of the Peierls-Fröhlich instability, one finds a gap equation directly analogous to the BCS gap equation with the implication that $E_g(T)$ should be of the BCS form.[42,43] The normalized BCS temperature dependence is shown for comparison in Fig. 7. The agreement is quite satisfactory at low temperatures, but the data appear to fall below the BCS curve above 30 K. The one-dimensional feature of the problem, however, suggests that fluctuations (beyond mean-field theory) should be important. Thus, the excess temperature dependence (above 30 K) may result from a fluctuation smearing of the gap. Direct optical measurements of the gap would be very helpful in establishing this point.

The microwave properties (g), (h), and (i) associated with the a axis are particularly interesting. Qualitatively, the large anisotropy in conductivity is consistent with the crystal structure as shown in Fig. 13. Transport along the a axis involves electron transfer between unlike (i.e., donor and acceptor) chains. Because of the small overlap and molecular inequivalence, one would anticipate this to be the lowest conductivity axis.

In attempting to understand these data, the first question to be answered is whether the conductivity

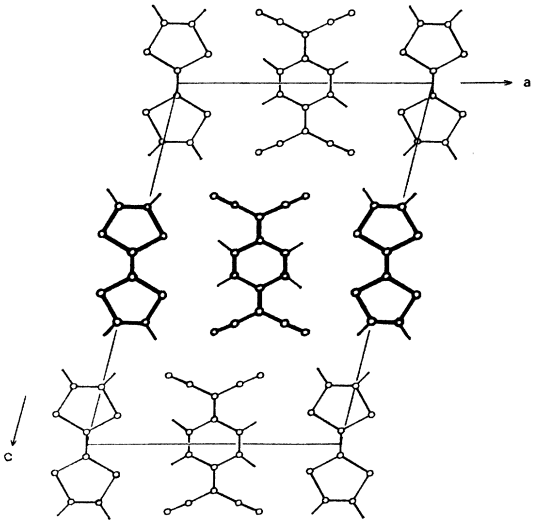

FIG. 13. X-ray crystal structure of TTF-TCNQ from the work of Ref. 3.

is intrinsic to the TTF-TCNQ system or results from defects. In highly anisotropic conductors, defects and dislocations can lead to effective interchain "shorts" which dominate the transverse conductivity. For example, in the dichalcogenide layered structures the transverse (interplane) conductivity has been demonstrated to be defect limited, and in special cases the particular screw-dislocation defect has been identified with electron microscopy.[44] However, there are several aspects of the a-axis data presented above which suggest that the conductivity is in fact intrinsic. The a-axis conductivity is temperature dependent going through a maximum at approximately 75 K. Since this temperature is considerably above the b-axis peak temperature (~60 K), the observed temperature dependence cannot be attributed to interchain shorts with b-axis conductivity between defects. Second, the magnitude and temperature dependence of $\sigma_1^a(T)$ as measured at dc and 10 GHz are in agreement. Finally, transport along the a axis is from TCNQ chains to TTF chains, etc. Whereas one might expect misplaced molecules to connect *like* chains, from a chemical and steric point of view it is much less likely that unlike chain contact will result. In what follows we therefore assume that the measured a-axis conductivity and dielectric constant are intrinsic.

Although the low-temperature dielectric constant follows directly from the anisotropic small-gap semiconductor (i.e., Peierls insulator) as described above, the signs and magnitudes of $\epsilon_1^a(T)$ and $\sigma_1^a(T)$ in the "metallic" regime present a fascinating problem. From the crystal structure and general electronic properties of TTF-TCNQ, we expect the tight-binding transfer integrals asso-

ciated with *interchain* coupling to be small. Thus the bandwidth associated with wave vectors along the a axis ($\vec{k}_a$) should be much less than that associated with the b axis, and the effective mass correspondingly anisotropic. As a rough measure of this anisotropy one can use the anisotropy in the conductivity, i.e., greater than 500 at room temperature. Although a crude estimate, this suggests the bandwidth associated with $\vec{k}_a$ (W_a) is of the order of 500 times narrower than that associated with the principal conducting (b) axis (W_b). Using the results obtained from the plasma frequency,[6-8] the susceptibility,[20] and the thermoelectric power,[13] we have $W_b \simeq 0.5$ eV, so that $W_a \sim 10$ K. Transport in such a narrow band (i.e., $W_a < k\Theta_D$, where Θ_D is the Debye temperature) is not metallic but diffusive and severely limited by the phonon thermal disorder. That a diffusion-theory approach to the transverse conductivity is necessary can be seen from an estimate of the mean free path along the a axis. Using the measured conductivity and the known electron density, one estimates from tight-binding theory $\lambda < 0.01$ Å, i.e., much less than a lattice constant, implying that the carriers do not propagate as in a metal but remain on a given site for relatively long times.

In this interesting case, the transverse transport properties must be calculated from diffusion theory. The conductivity is given by

$$\sigma_\perp^a = N_{eff} e \mu^a , \tag{13}$$

where N_{eff} is the effective number of carriers and μ^a their mobility along the a axis. Since we are dealing with a degenerate electron system, $N_{eff} = N(0) k_B T$, where $N(0)$ is the density of states at the Fermi energy. From standard diffusion theory we may write the Einstein mobility as

$$\mu^a = eD/k_B T , \tag{14}$$

where e is the electron charge, and D the diffusion constant. Since we are assuming the phonon thermal disorder is the source of the diffusive transport, we may write

$$D = \nu_D a^2 (t_\perp^a/\gamma \langle u^2 \rangle^{1/2}) , \tag{15}$$

where ν_D is the typical phonon frequency (of order the Debye frequency) and a is the appropriate lattice constant. The quantity in brackets represents the probability of an intermolecular hop given the fact that ν_D times per second the levels on neighboring sites becomes degenerate. This probability is given by the ratio of the interchain transfer integral $t_\perp^a$ to the strength of the effective electron-phonon (el-ph) random potential,

$$V_{\text{el-ph}}^{\text{random}} \simeq \gamma \langle u^2 \rangle^{1/2} , \tag{16}$$

where γ is the electron-phonon coupling constant and $\langle u^2 \rangle^{1/2}$ is the rms displacement of the molecules from their equilibrium positions. From standard Debye theory we may write[45]

$$\langle u^2 \rangle^{1/2} = (9\hbar^2 T/M k_B \Theta^2)^{1/2} , \tag{17}$$

where T is the temperature, M is the molecular mass, and Θ the Debye temperature. Since the dominant source of electron-phonon interaction is expected to arise from modulation of the Madelung and polarization contributions to the cohesive energy,[4] we anticipate that $\gamma \simeq 1$ eV/(lattice constant) $\sim 10^7$ eV/cm. Substituting Eqs. (14), (15), and (17) into Eq. (13) leads to the following expression for the transverse conductivity:

$$\sigma_\perp^a = \frac{2Ne^2 \nu_D a^2}{\pi E_F} \left(\frac{M k_B \Theta^2}{9\hbar^2} \right)^{1/2} \left(\frac{t_\perp^a}{\gamma} \right) \frac{1}{T^{1/2}} . \tag{18}$$

All quantities in Eq. (18) are known for TTF-TCNQ with the exception of $(t_\perp^a/\gamma)$, and we have a reasonable estimate of γ based on our understanding of the electron-phonon interaction in such ionic and polarizable metals.

The $T^{-1/2}$ dependence is shown for comparison with the data as the dashed curve in Fig. 11. The agreement is reasonable, although the experimental data do fall somewhat more rapidly at higher temperatures (a best-fit power law yields $T^{-0.7}$). The dashed curve in Fig. 11 assumes $\sigma = AT^{-1/2}$, with $A \simeq 8.8\ (\Omega\,\text{cm})^{-1}\,\text{K}^{1/2}$. A theoretical estimate can be obtained in a straightforward manner. For TTF-TCNQ we have $N = 4.7 \times 10^{21}$, $E_F \simeq 0.25$ eV, $\Theta \simeq 10^2$ K, and $M \simeq 3.3 \times 10^{-22}$ g. The remaining unknown is the ratio $(t_\perp^a/\gamma)$. To fit the experimental results requires $(t_\perp^a/\gamma) \simeq 5 \times 10^{-10}$ cm. From the discussion of Sec. III on the low-temperature dielectric constant ϵ_1^a and measurements of the anisotropy in conductivity, one estimates $t_\perp^a \simeq 10^{-3}$ eV (10 K), so that $\gamma \simeq 2 \times 10^6$ eV/cm; e.g., of the expected order of magnitude. Of course at low temperatures, where an energy gap opens in the electronic spectrum, these ideas become inapplicable and an exponentially small transverse conductivity is expected and observed.

The random effective potential given in Eq. (16) thus causes a severely inhibited diffusive transport. In effect, therefore, this random potential represents a restoring force to electron motion and can be expected to dominate the transverse dielectric response. Carrying this analysis further we expect

$$\epsilon_1^a \simeq 1 + (\omega_p^a/\omega_0)^2 , \tag{19}$$

where $(\omega_p^a)^2$ describes the transverse oscillator strength [$(\omega_p^a)^2 = 16Ne^2 t_\perp^a a^2/\hbar^2$ in tight binding] and $\hbar\omega_0 \equiv \gamma \langle u^2 \rangle^{1/2}$. As a result, using Eq. (17),

$$\epsilon_1^a \simeq 1 + \frac{16Ne^2 t_\perp^a a^2 M k_B \Theta^2}{9\gamma^2 \hbar^2 T} . \tag{20}$$

The T^{-1} dependence is readily seen in the experi-

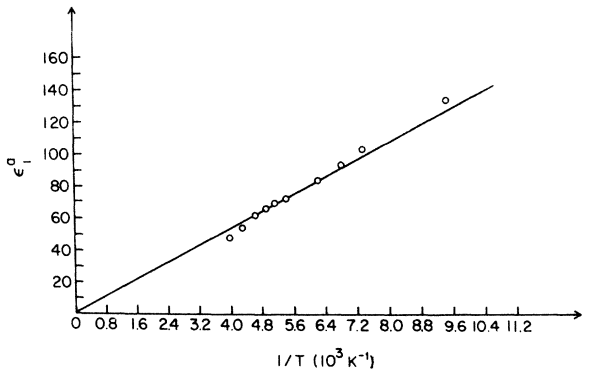

FIG. 14. a-axis dielectric constant (ϵ_1^a) versus inverse temperature (T^{-1}).

mental data as shown in Fig. 14. From the slope (assuming $t_\perp^a \simeq 10^{-3}$ eV as obtained above) one finds $\gamma = 3\times 10^6$ eV/cm, in excellent agreement with the value obtained from the diffusion conductivity.

A final comparison of Eqs. (18) and (20) and the experimental results can be made by noting that

$$\frac{(\sigma_\perp^a)^2}{\epsilon_1^a} = N t_\perp^a \left(\frac{ea\nu_D}{2\pi E_F}\right)^2 . \tag{21}$$

Thus, the ratio $(\sigma_\perp^a)^2/\epsilon_1^a$ depends only on the known parameters of the system, and is independent of temperature. Evaluating Eq. (21), one obtains $(\sigma_\perp^a)^2/\epsilon_1^a \sim 10^{21}$ esu in comparison with the experimental results as shown in Fig. 15. The experimental ratio varies little throughout the "metallic" regime and has a value in rough agreement with the above estimate.

V. CONCLUSION

We have presented a study of the anisotropic microwave conductivity and dielectric constant for TTF-TCNQ as a function of temperature. Above 60 K, the results indicate a highly anisotropic (pseudo-one-dimensional) metal. The measurements associated with the a axis (transverse to the principal conducting b axis) are consistent with a very weak interchain coupling and diffusive transport.

The transport properties of the one-dimensional coupled electron-phonon system have been the subject of considerable current interest. Although it is generally agreed that the giant density wave conductivity mechanism proposed by Fröhlich[10] in 1954 would be subject to a variety of pinning mechanisms,[39,46] pseudo-one-dimensional systems like TTF-TCNQ are prime candidates for seeing such effects. Allender, Bray, and Bardeen[12] have estimated a fluctuation conductivity near the mean-field transition of roughly 20 times the room-temperature value, and speculated that such effects would be pinned well below T_c with possibly excess microwave conductivity.[9] Lee, Rice, and Anderson[39] have considered such a system well below the mean field T_c and shown that one should expect an unusually large dielectric constant as well as excess microwave conductivity. Their expression for ϵ is given by[39]

$$\epsilon(0,\omega) = 1 + \frac{2}{3}\left(\frac{\omega_p}{\omega_G}\right)^2 + \frac{4\pi ne^2/M^*}{\omega_T^2 - \omega(\omega + i/\tau)}, \tag{22}$$

where we have inserted the phenomenological imaginary part via the relaxation time τ. ω_T is the pinning frequency in their model which may be intrinsic (interchain Coulomb coupling) or due to charged impurities, and M^* is the effective mass associated with the coupled electron-phonon running wave.

The dielectric constant (b axis) reported here is unusually large, and it is tempting to try to make contact with Eq. (22). However, as we demonstrated above, the single-particle contribution expected for a direct small-band-gap one-dimensional semiconductor [Eq. (11)] is sufficient to account for the data so that the pinning contribution might not dominate. The excess microwave conductivity described in Sec. III could be related to the imaginary part of Eq. (22), especially since it appears to be largest in the purest samples, but a more extensive frequency dependence is required before such interesting speculations can be considered seriously. A study of the frequency dependence is in progress.

There appear to be two energy gaps in the system at low temperatures: the first of order 0.14 eV[47] (present even at room temperature), and the second of order 0.01 eV associated with the low-temperature metal-insulator transition. Our current understanding is that the two gaps are in the excitation spectrum of the two chains. The smaller

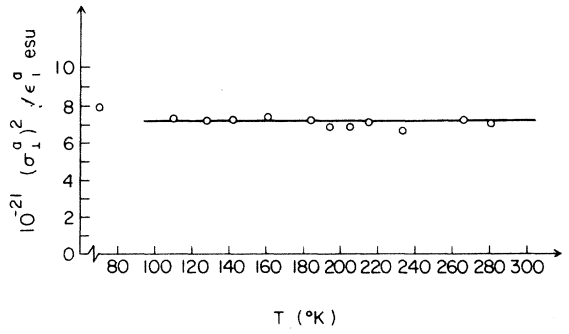

FIG. 15. $(\sigma_\perp^a)^2/\epsilon_1^a$ versus temperature (T).

gap (if direct) would dominate the dielectric constant as suggested in Eq. (11). However, there is evidence in the far infrared[47] of the collective mode implied in Eq. (22) which may well dominate both the low-temperature dielectric constant and the microwave losses.

The measurements reported in this paper provide no direct evidence relating to the giant conductivity peak observed in TTF-TCNQ.[1,15] The comparison of the microwave data presented here with that of Bloch *et al.*[26] explicitly demonstrates that trace impurities can significantly lower the b-axis conductivity as expected for a pseudo-one-dimensional metal. However, the Buravov-Shchegolev analysis employed in the present studies becomes inapplicable for conductivities exceeding $10^4\,(\Omega\,\mathrm{cm})^{-1}$, and a treatment of the data appropriate to the skin-depth-limited regime is required.

The extreme anisotropy, $\sigma_{\parallel}^{b}/\sigma_{\perp}^{a}\sim 10^4$ in the vicinity of 60 K, does have serious implications on attempts to measure the intrinsic b-axis conductivity. The large anisotropy implies that the potential difficulties arising from inhomogeneous current distributions must be carefully considered. On the other hand, this anisotropy indicates that crystal purity and perfection are required at the level of parts per million, for defects on the scale of one in every 10^4 molecules along a chain could easily limit the b-axis conductivity.

ACKNOWLEDGMENTS

We thank Dr. Arnold Denenstein for help with the design and construction of the microwave apparatus. We are grateful to M. J. Cohen and L. B. Coleman for the use of the a-axis dc conductivity data prior to publication, and to L. B. Coleman for providing the x-ray crystal orientation data. We acknowledge several important discussions with Dr. F. G. Yamagishi, Dr. A. A. Bright, and Dr. J. Gulley. We thank Paul Nigrey and S. Goldberg for careful sample preparation. One of us (A. F. G.) expresses gratitude for a DuPont Young Faculty Grant.

APPENDIX: DIELECTRIC CONSTANT OF A SMALL-GAP ONE-DIMENSIONAL SEMICONDUCTOR

We consider a direct small-band-gap one-dimensional semiconductor in which the underlying molecular (or atomic) distribution differs only slightly from the uniform chain. Since the systems of interest are characteristically narrow-band solids, it is appropriate to use tight-binding theory. The Hamiltonian is assumed to be

$$H = H_0 + V, \tag{A1}$$

where H_0 represents the uniform chain, and

$$H_0\psi_k(r) = E_0(k)\psi_k(r), \tag{A2}$$

with

$$E_0(k) = 2t(1-\cos ka), \tag{A3}$$

and

$$\psi_k(r) = \frac{1}{\sqrt{N}}\sum_j \varphi(r-r_j)e^{ikr_j}.$$

Here t is the transfer integral and $\varphi(r)$ is the normalized molecular wave function. $V(r)$ is a weak periodic perturbation potential with period $b=\pi/k_F$, where k_F is the Fermi wave number. The Hamiltonian (A1) is therefore that of a small-band-gap one-dimensional semiconductor.

For simplicity we assume 1 electron per molecule; i.e., $k_F=\pi/2a$ and $b=2a$. The total Hamiltonian satisfies

$$H\varphi_k(r) = E(k)\varphi_k(r). \tag{A4}$$

For a weak perturbation we assume, as in nearly-free-electron theory,

$$\varphi_k = \alpha_k\psi_k + \alpha_{k-G_1}\psi_{k-G_1}, \quad \alpha_k^2+\alpha_{k-G_1}^2 = 1, \tag{A5}$$

where $G_1=2\pi/b$, the reciprocal-lattice vector of the distorted crystal. Solving the coupled equations leads to

$$E^{\pm}(k) = \tfrac{1}{2}(\epsilon_0(k)+\epsilon_0(k-G_1) \pm \{[\epsilon_0(k)-\epsilon_0(k-G_1)]^2+4\,|V_{k,k-G_1}|^2\}^{1/2})$$

and

$$\frac{\alpha_k^{\pm}}{\alpha_{k-G_1}^{\pm}} = \frac{E^{\pm}(k)-E_0(k-G_1)}{V_{k,k-G_1}}, \tag{A6}$$

where

$$V_{k,k'} = \int \psi_k^*(r)V(r)\psi_k(r)\,dr \tag{A7}$$

and $\epsilon_0(k)=E_0(k)+V_{k,k'}$. The superscripts $\pm$ refer to the cases $|k|>k_F$ (upper band) and $|k|<k_F$ (lower band). In the tight-binding limit, i.e.,

$$\int |\varphi(r-r_j)|^2 V(r)\,dr \gg \int \varphi^*(r-r_j-a)V(r)\varphi(r-r_j)\,dr,$$

$V_{k,k'}$ depends only on the difference $|k-k'|$. The minimum energy gap is $E_G=2|V_{G_1}|\equiv 2|V_{k,k-G_1}|$ and there is the usual $1/\sqrt{\epsilon}$ singularity in density of states near the gap edges characteristic of a one-dimensional system.

The frequency- and wave-number-dependent dielectric constant in the self-consistent-field theory is given by[48,49]

$$\epsilon(\omega,q) = 1-\frac{4\pi e^2}{q^2}\sum_{k,l,l'}|M(k,q,l,l')|^2 \times\frac{f(E^{l'}(k+q))-f(E^{l}(k))}{E^{l'}(k+q)-E^{l}(k)-\hbar\omega}, \tag{A8}$$

where l, $l'=+$ or $-$ are the band indices, f is the

Fermi distribution function, and $M(k, q, l, l') = \int \varphi_k^{l*}(r) e^{-iqr} \varphi_{k+q}^{l'} dr$. To obtain explicit expressions for $\epsilon(\omega, q \approx 0)$ we have to evaluate the matrix element M. Using Eq. (A5) one finds, for $q \approx 0$,

$$M(k, q, l, l') = \langle k, l | e^{-iqr} | k+q, l' \rangle , \tag{A9}$$

$$= (\alpha_k^l \alpha_{k+q}^{l'} + \alpha_{k-G_1}^l \alpha_{k+q-G_1}^{l'}) C_q + (\alpha_k^l \alpha_{k+q-G_1}^{l'} + \alpha_{k-G_1}^l \alpha_{k+q}^{l'}) \hat{C}_q , \tag{A10}$$

where for extreme tight binding one can show that

$$C_{q=0} \approx 1 , \quad |\hat{C}_{q=0}| \approx (1/N) C_{q=0} . \tag{A11}$$

Using Eq. (A11) and ignoring the second term in Eq. (A10), we find for $q \to 0$

$$M(k, q, l, l') = \frac{1 + (4/E_G^2)[E^l(k) - \epsilon^0(k - G_1)][E^{l'}(k+q) - \epsilon^0(k+q-G_1)]}{(\{1 + (4/E_G^2)[E^l(k) - \epsilon^0(k-G_1)]^2\}\{1 + (4/E_G^2)[E^{l'}(k+q) - \epsilon^0(k+q-G_1)]^2\})^{1/2}} . \tag{A12}$$

For $l = l'$ Eq. (A12) yields $M \simeq 1$ as expected. For $l \neq l'$ the result is more complicated. The value of M is largest ($= tqa/E_G$) at the edge of the Brillouin zone where the admixture of the states at k and $k - G_1$ is the largest ($|\alpha_k|^2 = \frac{1}{2}$). This value decreases to a minimum $[\sim (E_G/t)(qa)^2]$ at $k = 0$ where the admixture is minimal as described by (A12).

Using (A12), the dielectric constant (A8) becomes

$$\epsilon(\omega, q \approx 0) = 1 - \frac{4\pi e^2}{q^2} \sum_{k, l} \frac{f(E^l(k+q)) - f(E^l(k))}{E^l(k+q) - E^l(k) - \hbar\omega} - \frac{4\pi e^2}{q^2} \sum_{k, l \neq l'} |M(k, q, l, l')|^2 \times \frac{f(E^l(k+q)) - f(E^{l'}(k))}{E^l(k+q) - E^{l'}(k) - \hbar\omega} \tag{A13}$$

$$= 1 + \epsilon_{\text{intra}} + \epsilon_{\text{inter}} . \tag{A14}$$

The second term on the right-hand side is readily evaluated, and in the limit $q \to 0$ is given by

$$\epsilon_{\text{intra}} = -\left(\frac{\omega_p^*}{\omega}\right)^2 \frac{\sum_k f(E^*(k))[\partial^2 E^*(k)/\partial k^2]}{\sum_k [\partial^2 E^0(k)/\partial k^2]} , \tag{A15}$$

where

$$(\omega_p^*)^2 = 4\pi e^2 \hbar^{-2} \sum_k \frac{\partial^2 E^0(k)}{\partial k^2} \tag{A16}$$

is the plasma frequency of a metal described by the Hamiltonian H_0, and the summation extends from $-\pi/b \leq k \leq \pi/b$. In the low-frequency region of interest to us ($< 10^{10}$ sec^{-1}), the finite electronic relaxation time τ must be taken into account. The ω^2 in the denominator of Eq. (A15) is to be replaced then by $(\omega^2 + 1/\tau^2)$, and the contribution of the intraband term is given by

$$\epsilon_{\text{intra}} = -\frac{(\omega_p^*)^2 \tau^2}{1 + \omega^2 \tau^2} \frac{\sum_k f(E^*(k))[\partial^2 E^*(k)/\partial k^2]}{\sum_k [\partial^2 E^0(k)/\partial k^2]} . \tag{A17}$$

The third term on the right-hand side of Eq. (A13) cannot be put in closed form because of the relatively strong q dependence of the matrix elements (A12). We have evaluated this term numerically, and for $t/E_G \gg 1$ the interband contribution can be parametrized as

$$\epsilon_{\text{inter}} = 0.65(\hbar\omega_p^*/E_G)^2 . \tag{A18}$$

The quantity ω_p^* is the plasma frequency of the tight-binding metal as given in Eq. (A16), and can be written as

$$(\omega_p^*)^2 = 4\pi N e^2/m^* , \tag{A19}$$

where

$$\frac{1}{m^*} = \hbar^{-2} \sum_k \frac{\partial^2 E^0(k)}{\partial k^2} = \frac{4ta^2}{\pi\hbar^2} . \tag{A20}$$

The quantity E_G is precisely the minimum direct band gap.

Note that at low temperatures, $k_B T < E_G$, the intraband contribution (A17) at low frequencies is of order $(\omega_p^* \tau)^2 e^{-E_G/k_B T}$ and is negligible. Consequently we expect the low-temperature dielectric constant for such a system to be given by

$$\epsilon_1 = 1 + 0.65[(\omega_p^*)^2/\omega_G^2] . \tag{A21}$$

†Supported by the National Science Foundation through the Laboratory for Research on the Structure of Matter and GP-39303, and the Advanced Research Projects Agency through DAHC 15-72C-0174.

*Work submitted in partial fulfillment of the requirements for the Ph.D.

‡Permanent address: Physics Dept., Technion, Haifa, Israel.

[1] L. B. Coleman, M. J. Cohen, D. J. Sandman, F. G. Yamagishi, A. F. Garito, and A. J. Heeger, Solid State Commun. 12, 1125 (1973).

[2] J. Ferraris, D. O. Cowan, V. Walatka, Jr., J. H. Perlstein, J. Am. Chem. Soc. 95, 948 (1973).

[3] T. E. Phillips, T. J. Kistenmacher, J. P. Ferraris, and D. O. Cowan, Chem. Commun. 14, 471 (1973); J. J. Daly and F. Sanz (unpublished).

[4] A. F. Garito and A. J. Heeger, *Nobel Symposium on Collective Properties of Physical Systems*, edited by B. Lundquist and S. Lundquist (Academic, New York, 1974), p. 129.

[5]E. F. Rybaczewski, A. F. Garito, and A. J. Heeger, Bull. Am. Phys. Soc. 18, 450 (1973).
[6]A. A. Bright, A. F. Garito, and A. J. Heeger, Solid State Commun. 13, 943 (1973).
[7]A. A. Bright, Ph.D. dissertation (University of Pennsylvania, 1973) (unpublished).
[8]A. A. Bright, A. F. Garito, and A. J. Heeger, Phys. Rev. B 10, 1328 (1974).
[9]J. Bardeen, Solid State Commun. 13, 357 (1973).
[10]H. Fröhlich, Proc. R. Soc. A 223, 296 (1954).
[11]Yu. A. Bychkov, L. P. Gorkov, and I. E. Dzyaloshinskii, Zh. Eksp. Teor. Fiz. 50, 738 (1966) [Sov. Phys.-JETP 23, 489 (1966)].
[12]D. Allender, J. W. Bray, and J. Bardeen, Phys. Rev. B 9, 119 (1974).
[13]P. M. Chaikin, J. F. Kwak, T. E. Jones, A. F. Garito, and A. J. Heeger, Phys. Rev. Lett. 31, 601 (1973).
[14]D. E. Schafer, F. Wudl, G. A. Thomas, J. P. Ferraris, and D. O. Cowan, Solid State Commun. 14, 347 (1974).
[15]Marshall J. Cohen, L. B. Coleman, A. F. Garito, and A. J. Heeger, Phys. Rev. B 10, 1298 (1974).
[16]L. J. Buravov and I. F. Shchegolev, Prib. Tek. Eksp. 2, 171 (1971).
[17]D. S. Acker, R. J. Harder, W. R. Hertler, W. Mahler L. R. Melby, R. E. Benson, and W. E. Mochel, J. Am. Chem. Soc. 82, 6408 (1960).
[18]L. B. Coleman, J. A. Cohen, A. F. Garito, and A. J. Heeger, Phys. Rev. B 7, 2122 (1973).
[19]S. K. Khanna (unpublished).
[20]J. C. Scott, A. F. Garito, and A. J. Heeger, Phys. Rev. B (to be published). These data were presented at the International Conference on Magnetism, Moscos, 1973 (unpublished), and at the Gatlinburg Conference on Superconductivity and Lattice Instabilities, 1973 (unpublished).
[21]A. A. Bright, P. M. Chaikin, and A. R. McGhie, Phys. Rev. B (to be published).
[22]D. L. Coffen, J. Q. Chambers, D. R. Williams, P. E. Garrett, and N. D. Canfield, J. Am. Chem. Soc. 93, 2258 (1971).
[23]G. Kiesslich, Ph.D. dissertation (Universität Würzburg, 1968) (unpublished).
[24]F. Wudl, D. Wobschall, and E. J. Hufnagle, J. Am. Chem. Soc. 94, 672 (1972).
[25]J. H. Perlstein, J. P. Ferraris, V. V. Walatka, Jr., D. O. Cowan, and G. A. Candela, AIP Conf. Proc. 10, 1494 (1973).
[26]A. N. Bloch, J. P. Ferraris, D. O. Cowan, and T. O. Poehler, Solid State Commun. 13, 753 (1973).
[27]T. Wei, S. Etemad, A. F. Garito, and A. J. Heeger, Phys. Lett. A 45, 269 (1973).
[28]These crystals were obtained from the IBM group at San Jose. The material was known to be impure.
[29]G. Thomas, Gatlinburg Conference on Superconductivity and Lattice Instabilities, 1973 (unpublished).
[30]The materials preparations carried out by Bloch, Cowan, and co-workers did not include any of the following procedures: multiple-gradient sublimation of TTF and TCNQ, quadruple distillations of CH_3CN solvent, or handling of materials and reactions under inert Ar atmospheres [D. O. Cowan (private communication)]. These purification steps are routinely followed in our laboratory.
[31]J. A. Osborn, Phys. Rev. 67, 351 (1945).
[32]L. I. Buravov, M. L. Khidekel', I. F. Shchegolev, and E. B. Yagubskii, Zh. Eksp. Teor. Fiz. Pis'ma Red. 12, 142 (1970) [Sov. Phys.-JETP Lett. 12, 99 (1970)].
[33]R. M. Vlasova, A. I. Gutman, V. V. Kuzina, and A. I. Sherle, Fiz. Tverd. Tela 12, 3479 (1970) [Sov. Phys.-Solid State 12, 2979 (1971)].
[34]For a discussion and references, see C. P. Poole, *Electron Spin Resonance* (Interscience, New York, 1967), Chap. 20.
[35]We thank Y. Tomkiewicz for pointing out to us this lineshape anisotropy.
[36]See A. J. Epstein, S. Etemad, A. F. Garito, and A. J. Heeger, Phys. Rev. B 5, 952 (1972).
[37]S. K. Khanna, A. F. Garito, and A. J. Heeger (unpublished).
[38]M. J. Rice and S. Strässler, Solid State Commun. 13, 697 (1973); *ibid.* 13, 1389 (1973).
[39]P. A. Lee, T. M. Rice, and P. W. Anderson, Phys. Rev. Lett. 31, 462 (1973); Solid State Commun. 14, 703 (1974).
[40]E. F. Rybaczewski, E. Ehrenfreund, A. F. Garito, and and A. J. Heeger (unpublished). These data were presented at the Gatlinburg Conference on Superconductivity and Lattice Instabilities, 1973 (unpublished).
[41]See, for example, M. Pollak and T. H. Geballe, Phys. Rev. 122, 1742 (1961).
[42]C. G. Kuper, Proc. R. Soc. A 227, 214 (1955).
[43]M. J. Rice and S. Strässler, Solid State Commun. 13, 697 (1973).
[44]F. Gamble, seminar (University of Pennsylvania, 1973) (unpublished).
[45]J. M. Ziman, *Principles of the Theory of Solids* (Cambridge U.P., Cambridge, England, 1969), Chap. 2.
[46]J. R. Schrieffer, *Nobel Symposium on Collective Properties of Physical Systems*, edited by B. Lundquist and S. Lundqvist (Academic, New York, 1974), p. 142.
[47]D. B. Tanner, C. S. Jacobsen, A. F. Garito, and A. J. Heeger, Phys. Rev. Lett. 32, 1301 (1974).
[48]H. Ehrenreich and M. H. Cohen, Phys. Rev. 115, 786 (1959).
[49]D. Penn, Phys. Rev. 128, 2093 (1962).

(a)

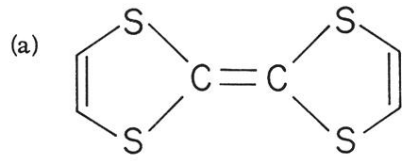

TTF

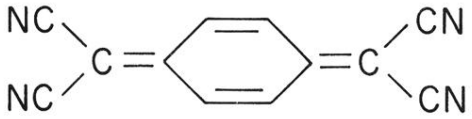

TCNQ

(b)

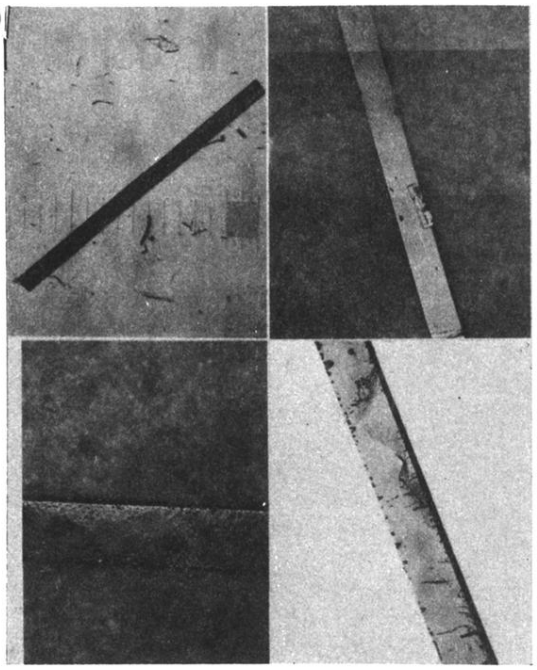

FIG. 1. (a) Molecular structure of TTF and TCNQ; (b) photographs of crystals of TTF-TCNQ having normal morphology with *b* axis parallel to crystal needle axis. The magnification is × 50 in the upper left, and × 100 for the other three.